Indonesian Journal of Interdisciplinary Research in Science and Technology (MARCOPOLO)
Vol. 4, No. 3, 2026: 167-186

Preparation of 1,2-Propanediol as Food Additives from Glycerol as Biodiesel By-product

Iffana Dani Maulida[1]*, Jumina[2]
[1]Department of Food Technology, Faculty of Science and Technology, Universitas Terbuka
[2]Department of Chemistry, Faculty of Mathematics and Natural Sciences, Universitas Gadjah Mada
Corresponding Author: Iffana Dani Maulida iffana@ecampus.ut.ac.id

A R T I C L E I N F O

Keywords: 1,2-Propanediol, glycerol; food additives; biodiesel

Received : 20, January
Revised : 24, February
Accepted: 28, March

A B S T R A C T

This study converts glycerol, a biodiesel by-product, into high-purity 1,2-propanediol for food additives. Utilizing a three-stage process—transesterification of palm oil, purification, and dehydration—structure confirmation was achieved using FTIR, ^{1}H-NMR, and GC-MS. Results indicated that transesterification yielded 10.38% crude glycerol, subsequently purified to 95.80%. Dehydration produced prop-2-en-1-ol (75.13%), eventually yielding 1,2-propanediol at 77.73% with 96.82% purity. Technical modifications, including dual distillation and optimized H_2: glycerol ratios (5:1) in simulation models, further enhanced purity to 99%. This research aligns with global sustainability trends and the FDA's 2026 priorities for safer food chemicals. The findings suggest that optimized 1,2-propanediol serves as a viable, non-toxic substitute for ethylene glycol, supporting the circular economy in food technology.

DOI: https://doi.org/10.55927/marcopolo.v4i3.30
E-ISSN: 2986-8009
https://journalmarcopolo.my.id/index.php/marcopolo

INTRODUCTION

Biodiesel production does not end cleanly with a tank of fuel; it also leaves behind glycerol as a major co-product, and that co-product is rarely equivalent to the refined polyol found on a laboratory shelf. Depending on the feedstock, alcohol-to-oil ratio, catalyst, washing procedure, and phase separation, crude glycerol can carry methanol, water, soaps, free fatty acids, inorganic salts, residual catalyst, methyl esters, and other non-glycerol organic matter. These impurities depress its market value and can interfere with any chemistry attempted on it downstream. Converting this stream into a higher-value molecule is therefore not simply a matter of finding a use for waste; it improves material efficiency across the biodiesel value chain and relieves the burden of low-value combustion or disposal. Recent reviews frame purification and catalytic upgrading not as separate downstream chores but as complementary stages of a single integrated glycerol biorefinery (Attarbachi et al., 2023;Rosmini et al., 2026)

One of the more attractive destinations for that upgraded glycerol is propane-1,2-diol (propylene glycol or 1,2-propanediol), it is a colorless, hygroscopic liquid already familiar to the food industry as a solvent, carrier, humectant, texture modifier, stabilizing aid, and processing ingredient. It is designated E1520 in the European Union and is affirmed as generally recognized as safe for specified uses in the United States. That regulatory comfort is not incidental; it rests on an accumulating body of toxicological reassessment emphasizing that exposure evaluation and compositional control must accompany functional performance, not substitute for it (Lewis et al., 2024; Tran et al., 2025).

The present work evaluates a laboratory pathway to that molecule which does not rely on a conventional hydrogenolysis catalyst. Glycerol recovered from palm-oil biodiesel is purified, converted to a product assigned as prop-2-en-1-ol, transformed into a formic ester through electrophilic addition of formic acid across its double bond, and finally hydrolyzed under alkaline conditions to 1,2-propanediol. The appeal of this sequence is chemical rather than merely economic: formic acid participates as a genuine reagent rather than a spectator, and the closing hydrolysis step regenerates the alcohol groups that give the final product its function. The experimental observations, yields, and spectra reported here are retained from the original study; the objective of this manuscript is to determine what that evidence does and does not establish regarding reaction identity, product purity, process sustainability, and readiness for food-additive use.

LITERATURE REVIEW

The dominant renewable route to 1,2-propanediol reported in the literature remains catalytic glycerol hydrogenolysis. Copper-based, nickel-based, noble-metal, and bifunctional catalysts have all been developed to activate glycerol while controlling C–O and C–C bond cleavage, and current reviews describe liquid-phase hydrogenolysis, vapor-phase hydrogenolysis, catalytic transfer hydrogenolysis, in-situ hydrogen generation, fermentation, and electrochemical approaches as competing or complementary pathways within

that same family (Okolie, 2022; Pandey & Biswas, 2023; Główka & Krawczyk, 2023; Ma et al., 2023). The prevailing mechanistic picture for this conventional route involves glycerol dehydration or dehydrogenation to reactive carbonyl intermediates, followed by hydrogenation to 1,2-propanediol, with catalyst acidity, metallic hydrogenation sites, water content, hydrogen pressure, and temperature all shaping conversion and selectivity. Copper-based catalysts are frequently favored because they promote C–O cleavage while limiting excessive C–C scission, and newer studies continue to optimize metal–support interactions, bimetallic compositions, oxygen vacancies, and multifunctional catalyst designs in pursuit of higher selectivity (H. Luo et al., 2014; Ghorbani et al., 2025; Hassenstein et al., 2026). What unites these routes, for all their differences, is a dependence on pressurized hydrogen, carefully engineered catalysts, or extensive downstream separation — requirements that raise the barrier to small-scale or laboratory adoption and that motivate the alternative, catalyst-free pathway examined in this manuscript.

Purification of the glycerol feedstock has received comparable attention because it directly limits what any downstream chemistry can achieve. Acidifying crude glycerol with a mineral acid neutralizes residual base, converts soaps into free fatty acids, and promotes phase separation, while the accompanying salts either precipitate out or remain dissolved in the aqueous glycerol phase. Because acidification alone does not remove every impurity, recent purification schemes combine it with evaporation, adsorption, membrane separation, ion exchange, or vacuum distillation, and purification performance is now expected to be reported in terms broader than glycerol percentage alone (residual water, ash, methanol, and organic non-glycerol) matter all shape downstream suitability (Attarbachi et al., 2023b). Life-cycle and techno-economic studies reinforce the same point from the process-engineering side: the best purification route depends on the purity grade required, the recovery achieved, the energy demand, and the chemical consumption involved, not on purity in isolation (Bansod et al., 2024; Bansod et al., 2025).

Taken together, this literature makes clear that food-additive suitability is not something that structural chemistry alone can settle. Structural confirmation establishes the identity of the major product; quantitative assay establishes how much of it is actually present; impurity profiling determines what travels alongside it; and specification testing determines whether the material clears a regulatory or compendial bar. These steps are related, but answering one does not answer the others. The theoretical evaluation that follows in this manuscript therefore rests on four criteria drawn directly from this body of work: the consistency of the reported spectra with the proposed structures, the adequacy of the reported chromatographic purity, the fit of the results with recent glycerol-valorization literature, and the gap that remains between a promising laboratory synthesis and a food-grade qualification.

METHODOLOGY

Palm oil was used as the triglyceride feedstock. Methanol, potassium hydroxide, sulfuric acid, formic acid, sodium hydroxide, anhydrous sodium

sulfate, dichloromethane, sodium bicarbonate, and ethanol were analytical-grade reagents. The principal equipment consisted of reflux and fractionating-distillation assemblies, an atmospheric distillation unit, heated magnetic stirring equipment, rotary evaporation, vacuum equipment, standard laboratory glassware, and analytical instruments for Fourier-transform infrared spectroscopy (FTIR), gas chromatography-mass spectrometry (GC-MS), and proton nuclear magnetic resonance spectroscopy (^{1}H NMR, 400 MHz).

Water was removed from 200 g of palm oil by heating at 110^{0}C for 30 min. Transesterification was carried out using KOH at 1% of the oil mass in methanol, with a methanol-to-oil molar ratio of 6:1, for 2 h at 70^{0}C under reflux. After settling, the lower crude-glycerol phase was separated. Sulfuric acid solution at 2.5% was added at 5% of the crude-glycerol mass to neutralize catalyst residues and convert soaps into free fatty acids. The fatty-acid fraction was removed by filtration, and volatile methanol and water were reduced by evaporation. The purified glycerol was characterized by FTIR, GC-MS, and ^{1}H NMR.

For the intermediate stage, 0.3 mol glycerol and 0.2 mol formic acid were subjected to fractional distillation. Early condensate was separated, and NaOH pellets were used to reduce acidic and aldehydic components in the receiver. Distillate fractions were collected as the temperature increased, with the main fraction collected near 225-235^{0}C and the operation stopped at 260^{0}C. Additional formic acid was introduced to the cooled residue and fractionation was repeated. The combined fractions were neutralized to approximately pH 6-7, dried with anhydrous sodium sulfate, and redistilled at approximately 97 0C. The product assigned as prop-2-en-1-ol was analyzed by FTIR, GC-MS, and ^{1}H NMR.

The isolated intermediate (0.1 mol) was refluxed with formic acid (0.4 mol) and three drops of sulfuric acid at 105^{0}C for 5 h. The mixture was extracted three times with dichloromethane, washed with cold water, neutralized with sodium bicarbonate, dried over anhydrous sodium sulfate, and concentrated. The resulting formic ester was assessed by FTIR. For hydrolysis, the ester was refluxed for 2 h with ethanolic KOH at a 1:2 ratio. The mixture was neutralized with sulfuric acid, extracted with dichloromethane, concentrated, and characterized by FTIR, GC-MS, and ^{1}H NMR.

RESEARCH RESULT

The transesterification step separated into an upper biodiesel-rich layer and a lower glycerol-rich layer after approximately 15 min of settling. Crude glycerol corresponded to 10.38% w/w of the palm-oil feed. Following evaporation and sulfuric-acid treatment, glycerol was recovered at a reported yield of 89.80%. The principal GC peak represented 95.80% of the total integrated chromatographic area. Whole sequence and principal analytical results are summarized in Table 1.

The reaction scheme in Figure 1 illustrates base-catalyzed transesterification of triglyceride with methanol. Methoxide attacks the ester carbonyl, producing methyl esters and stepwise conversion of triglyceride through di- and monoglycerides to glycerol. The use of excess methanol shifts the reversible reaction toward ester formation. In the recovered glycerol phase,

residual KOH and soap were expected to remain. Sulfuric acid neutralization converted alkaline residues into salts and protonated soaps to free fatty acids, which were removed as a separate fraction or by filtration.

Table 1. Summary of reported process performance and analytical evidence

Stage	Reported yield/recovery	Reported GC-area purity	Principal evidence
Crude glycerol recovery	10.38% w/w of oil feed	-	Phase separation after transesterification
Purified glycerol	89.80%	95.80%	FTIR, GC-MS, ^{1}H NMR
Prop-2-en-1-ol fraction	75.13%	83.66%	FTIR terminal-alkene bands, GC-MS, ^{1}H NMR
1,2-Propanediol fraction	77.73%	96.82%	Loss of ester C=O; GC-MS; methyl/methylene/methine ^{1}H NMR

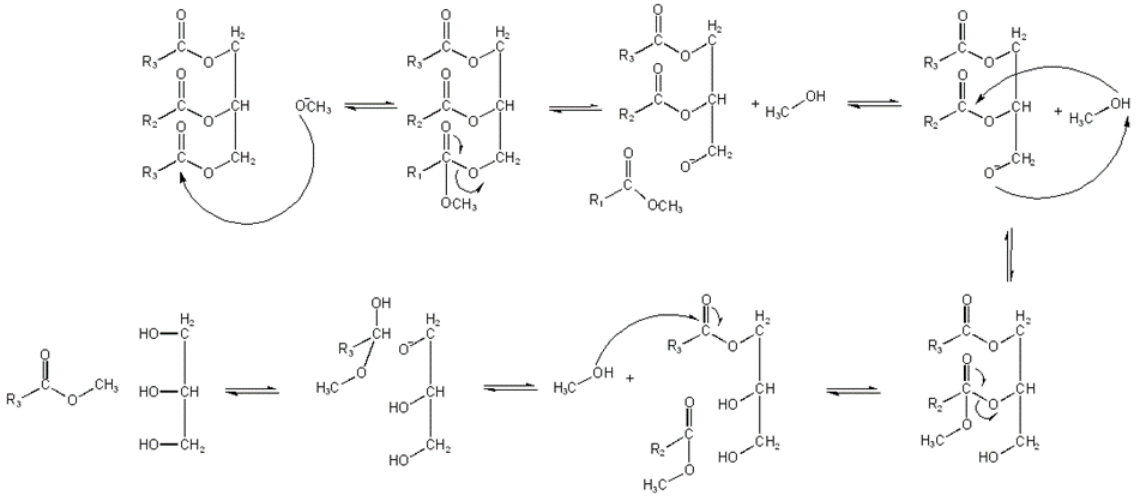

Figure 1. Proposed mechanism of triglyceride transesterification using a base catalyst

The FTIR spectrum of purified glycerol (Figure 2) showed a broad O-H stretching band at 3433 cm^{-1}, aliphatic C-H stretching at 2916 cm^{-1}, a band at 1643 cm^{-1} assigned principally to H-O-H bending from residual water, and C-H bending at 1411 cm^{-1}. The strong and broad hydroxyl envelope was consistent with a polyol. The 1643 cm^{-1} feature indicated that the material remained hygroscopic and that water was not completely removed. Table 2 lists the reported assignments.

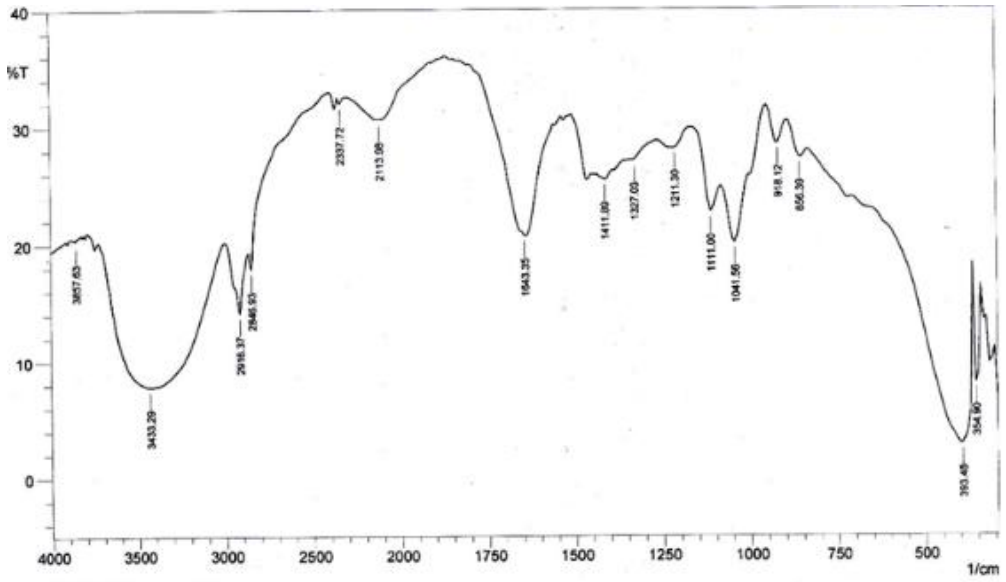

Figure 2. FTIR spectrum of purified glycerol

Table 2. Reported FTIR assignments for purified glycerol

Vibration	Wavenumber (cm^{-1})
O-H stretching	3433
C_{sp^3}-H stretching	2916
H-O-H bending	1643
C_{sp^3}-H bending	1411

The glycerol chromatogram (Figure 3) contained three peaks. The major peak at a retention time of 18.52 min accounted for 95.80% of the integrated area and was assigned to glycerol. The mass spectrum (Figure 4) did not show an intense molecular ion at m/z 92, while m/z 61 was the base peak. The observed fragmentation was considered consistent with glycerol under the selected electron-ionization conditions. The ^{1}H NMR spectrum (Figure 5) showed multiplets in the 3.49-3.65 ppm region assigned to methylene and methine protons, together with exchangeable hydroxyl-related signal intensity in the methanolic solvent.

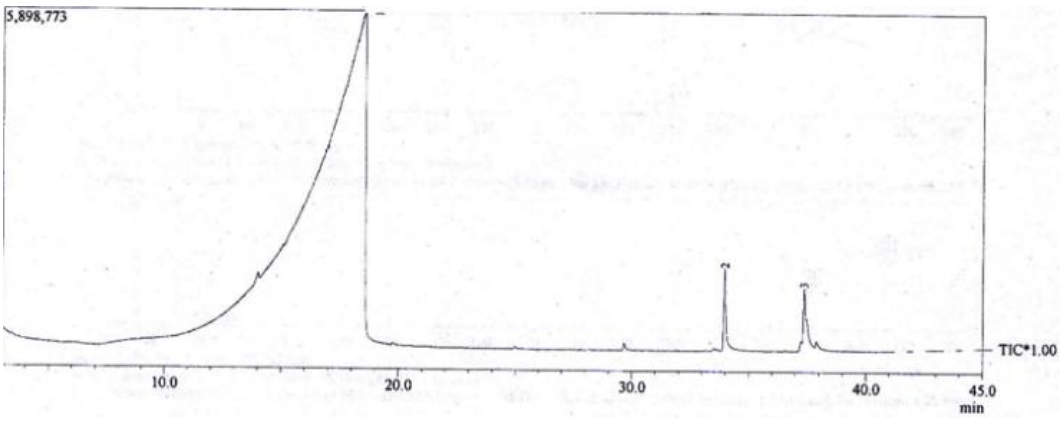

Figure 3. GC chromatogram of purified glycerol

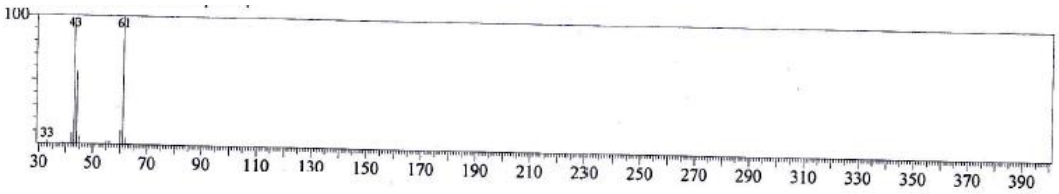

Figure 4. Mass spectrum of purified glycerol

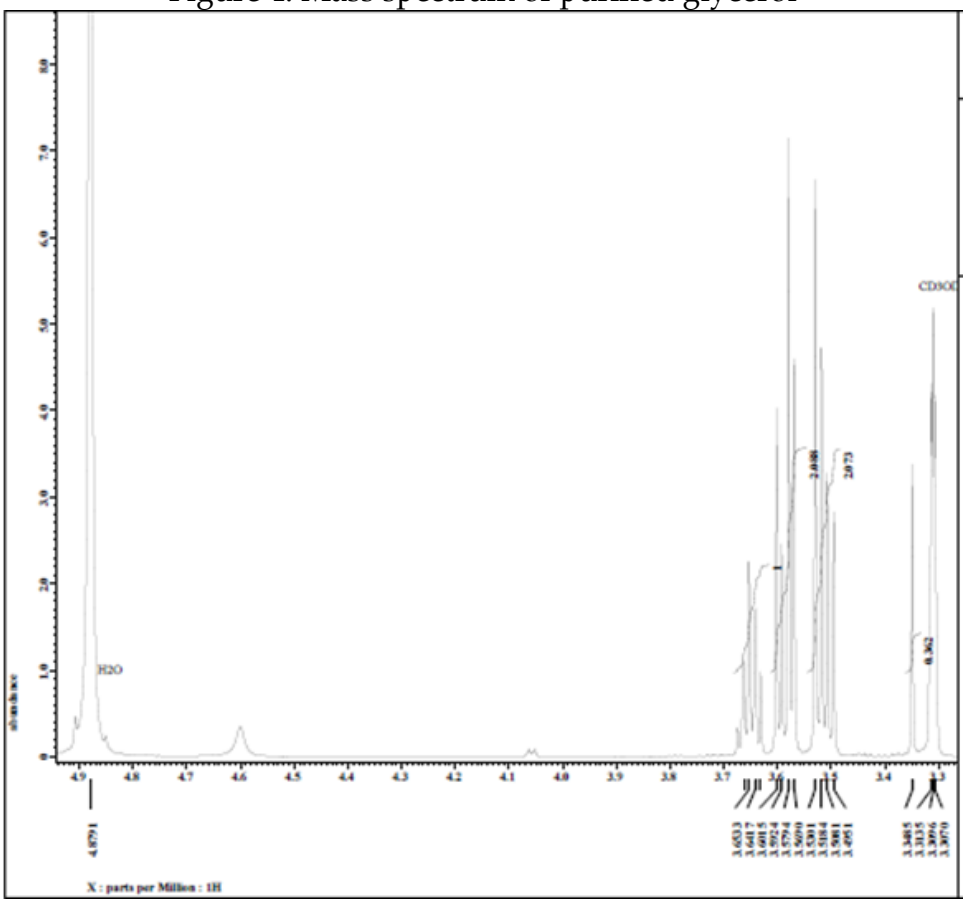

Figure 5. ^{1}H NMR spectrum of purified glycerol

Table 3. Reported ^{1}H NMR assignments for glycerol

Peak	Chemical shift (ppm)	Multiplicity	Assignment
a	3.49-3.53	Multiplet	4H, methylene
b	3.57-3.60	Multiplet	Hydroxyl-related signal
c	3.64-3.65	Multiplet	1H, methine

Fractional distillation of glycerol with formic acid yielded 75.13% of a product assigned as prop-2-en-1-ol. Its chromatographic area purity was 83.66%. Operationally, the temperature ramp was critical: prolonged heating was associated with darkening and increased formation of an aldehydic fraction, whereas insufficient heating reduced recovery of the desired volatile fraction. The reaction representation is shown in Figure 6. Because several glycerol-dehydration products can form at elevated temperature, the product assignment was evaluated using all three analytical techniques rather than boiling point alone.

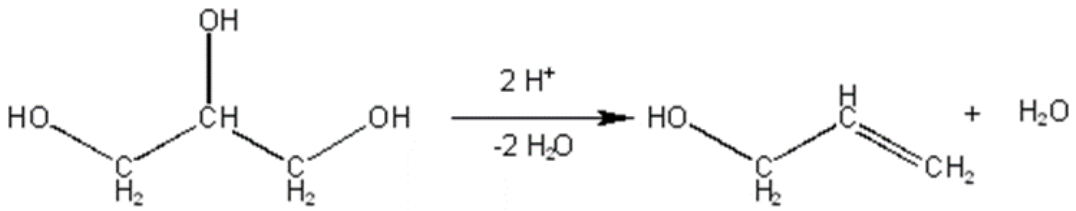

Figure 6. Proposed conversion of glycerol to the unsaturated-alcohol fraction

The intermediate FTIR spectrum (Figure 7) contained O-H stretching at 3394 cm^{-1}, a weak unsaturated C-H feature at 3093 cm^{-1}, aliphatic C-H stretching at 2924 cm^{-1}, a band at 1643 cm^{-1} assigned to C=C stretching, C-H bending at 1427 cm^{-1}, and vinyl out-of-plane bands at 995 and 922 cm^{-1}. Together, the 3093, 1643, 995, and 922 cm^{-1} features were consistent with a terminal alkene. The GC chromatogram (Figure 8) showed a principal peak at 2.38 min with 83.66% relative area, and the mass spectrum (Figure 9) showed a base peak at m/z 57.

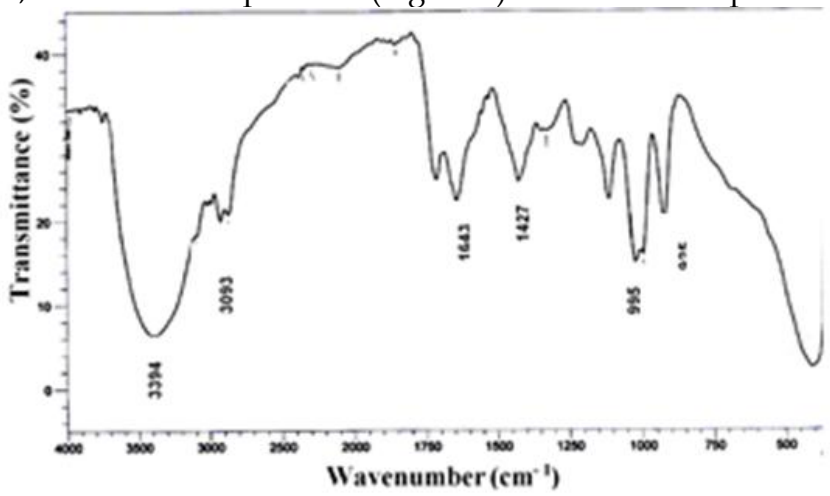

Figure 7. FTIR spectrum of the product assigned as prop-2-en-1-ol

Table 4. Reported FTIR assignments for prop-2-en-1-ol

Vibration	Wavenumber (cm^{-1})
O-H stretching	3394
C_{sp^2}-H stretching	3093
C_{sp^3}-H stretching	2924
C=C stretching	1643
C_{sp^3}-H bending	1427
Terminal vinyl bending	995 and 922

The ^1H NMR spectrum of the intermediate (Figure 10) contained a two-proton doublet at 4.16 ppm assigned to CH_2-OH, signals at 5.16 and 5.26 ppm assigned to the non-equivalent terminal-vinyl protons, and a signal near 6.00 ppm assigned to the internal vinyl proton. This pattern was qualitatively consistent with CH_2=CH-CH_2OH.

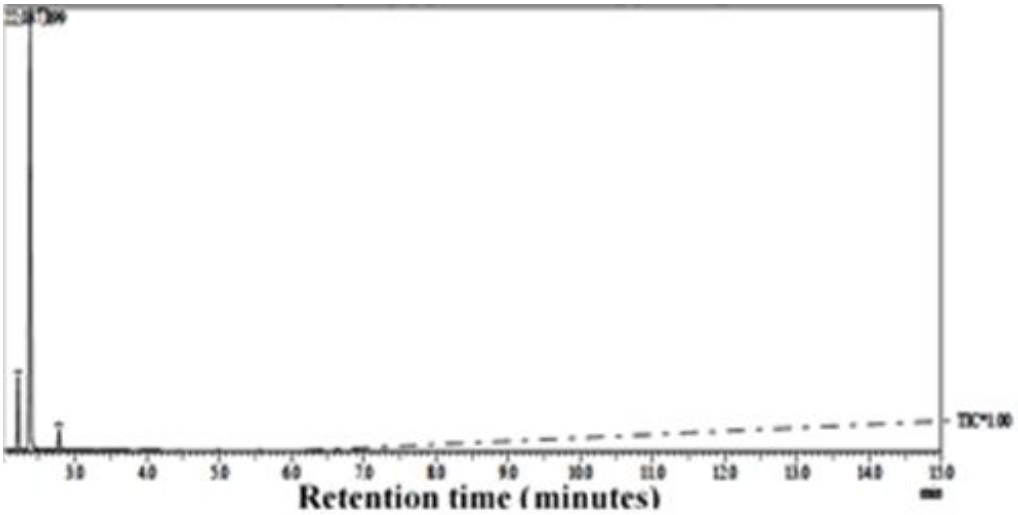

Figure 8. GC chromatogram of the product assigned as prop-2-en-1-ol

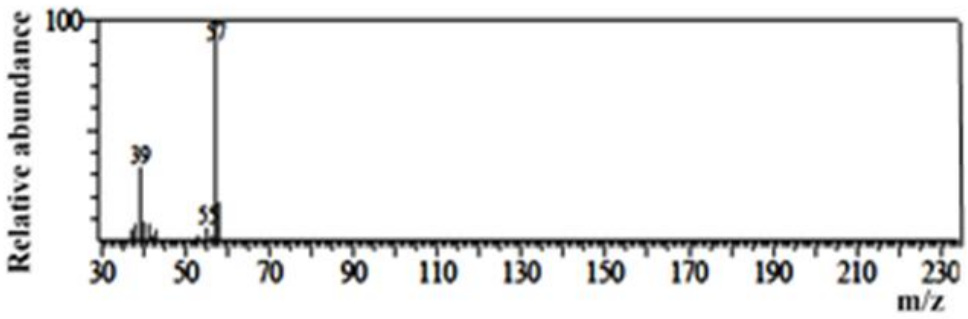

Figure 9. Mass spectrum of the product assigned as prop-2-en-1-ol

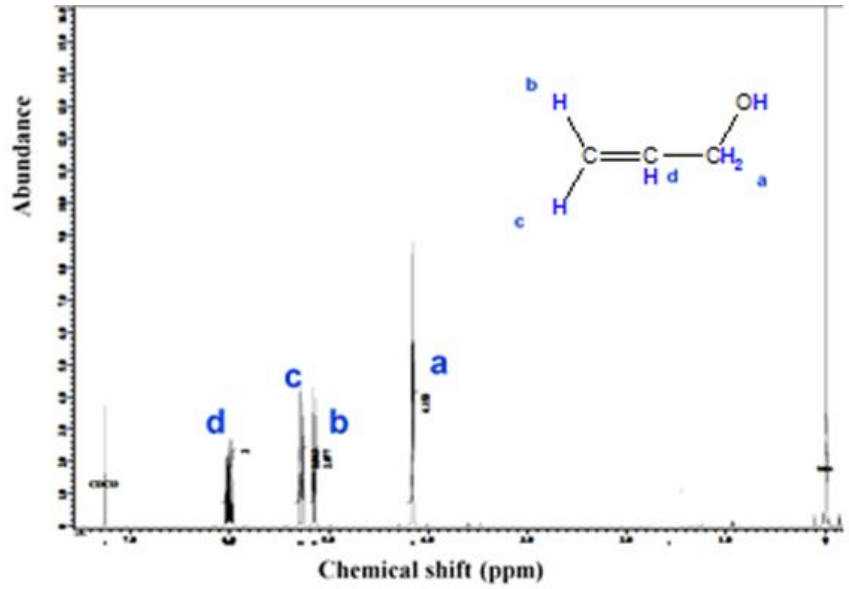

Figure 10. ^{1}H NMR spectrum of the product assigned as prop-2-en-1-ol

Table 5. Reported ^{1}H NMR assignments for prop-2-en-1-ol

Peak	Chemical shift (ppm)	Multiplicity	Assignment
a	4.16	Doublet	2H, =CH-CH_2-OH
b	5.16	Triplet	1H, terminal vinyl
c	5.26	Triplet	1H, terminal vinyl
d	6.00	Triplet	1H, internal vinyl

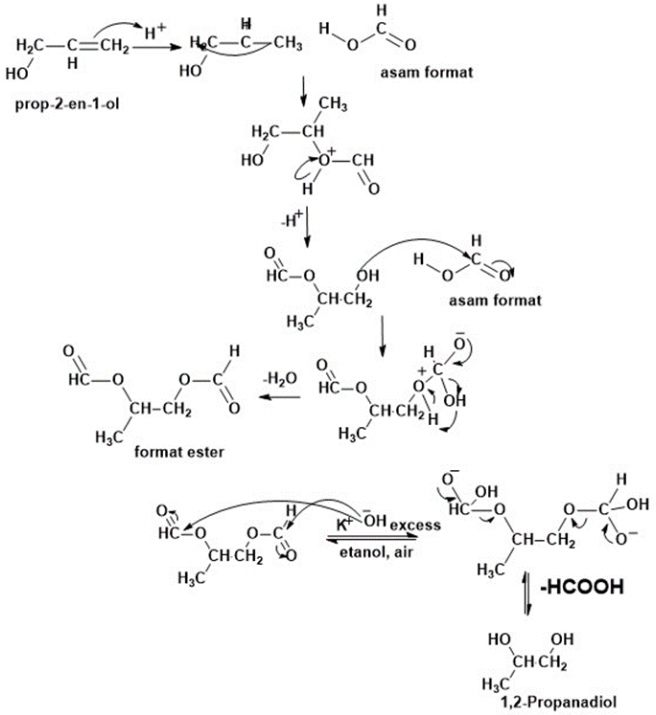

Figure 11. Proposed formation of 1,2-propanediol through formate addition and hydrolysis

Reaction of the unsaturated fraction with formic acid and catalytic sulfuric acid produced an ester-containing material. The FTIR spectrum (Figure 12) showed C-H stretching at 2939 cm^{-1}, C-H bending at 1427 cm^{-1}, a strong carbonyl band at 1728 cm^{-1}, and C-O ester stretching at 1172 cm^{-1}. Appearance of the carbonyl and ester C-O bands relative to the unsaturated alcohol was consistent with formate formation. The proposed electrophilic-addition and ester-hydrolysis sequence is illustrated in Figure 11.

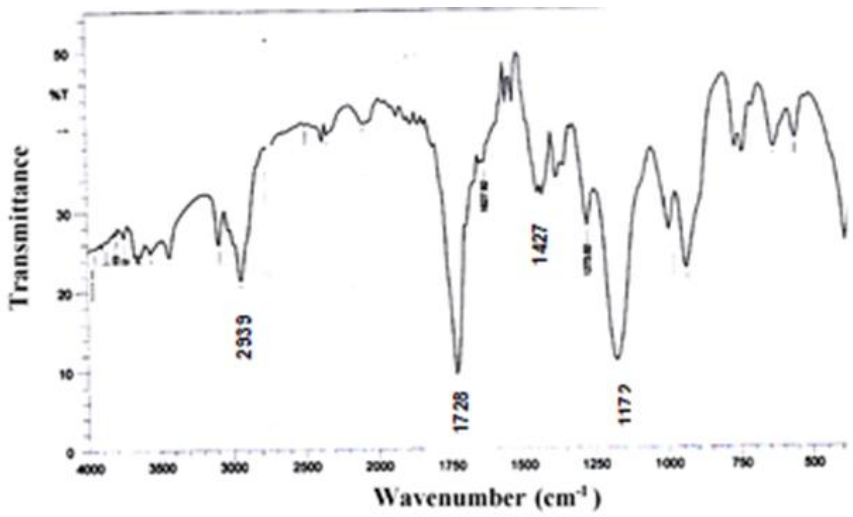

Figure 12. FTIR spectrum of the formic-ester fraction

Table 6. Reported FTIR assignments for the formic-ester fraction

Vibration	Wavenumber (cm^{-1})
C_{sp^3}-H stretching	2939
C_{sp^3}-H bending	1427
C=O stretching	1728
C-O ester stretching	1172

Alkaline hydrolysis of the ester-containing product gave a colorless fraction assigned as 1,2-propanediol at a reported yield of 77.73%. The FTIR spectrum (Figure 13) showed broad O-H stretching at 3379 cm^{-1}, C-H stretching at 2970 and 2877 cm^{-1}, C-H bending at 1411 cm^{-1}, and C-O stretching bands at 1049 and 1288 cm^{-1}. The strong ester carbonyl at 1728 cm^{-1} was absent, indicating substantial conversion of the formate functionality. The result was consistent with regeneration of alcohol groups during saponification.

Table 7. Reported FTIR assignments for 1,2-propanediol

Vibration	Wavenumber (cm^{-1})
O-H stretching	3379
O-H bending	1134
C_{sp^3}-H stretching	2970 and 2877
C_{sp^3}-H bending	1411
C-O alcohol stretching	1049 and 1288

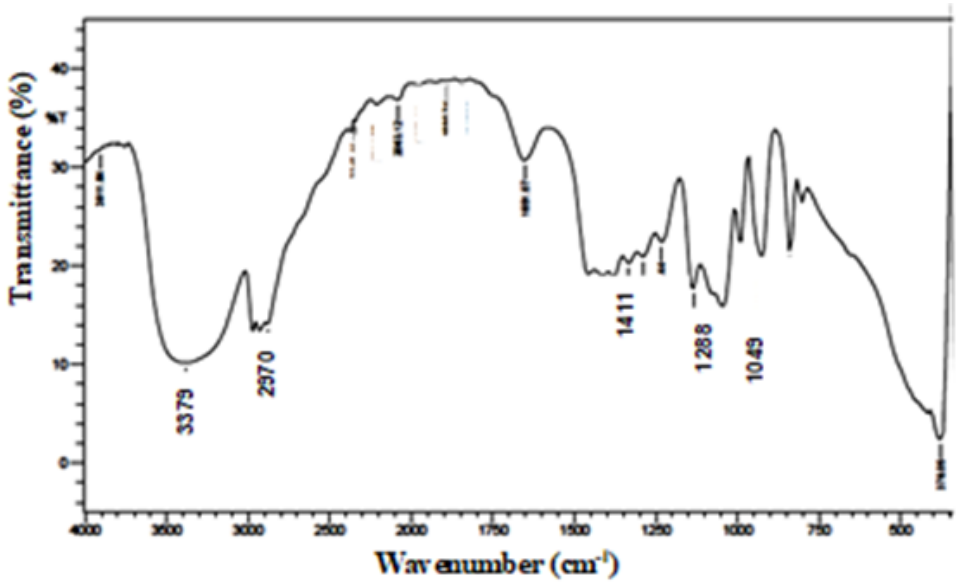

Figure 13. FTIR spectrum of the final 1,2-propanediol-rich fraction

The final GC chromatogram (Figure 14) showed a main peak at 3.86 min representing 96.82% of total integrated area. The mass spectrum (Figure 15) exhibited the expected extensive fragmentation of a small diol rather than a dominant molecular ion. The ^{1}H NMR spectrum (Figure 16) contained a methyl doublet at 1.14 ppm, a methylene signal at 3.41 ppm, a methine multiplet at 3.74-3.78 ppm, and an exchangeable signal near 4.90 ppm. The methyl doublet coupled to a neighboring methine and the oxygenated methylene/methine region were consistent with CH_3-CH(OH)-CH_2OH (Figure 16).

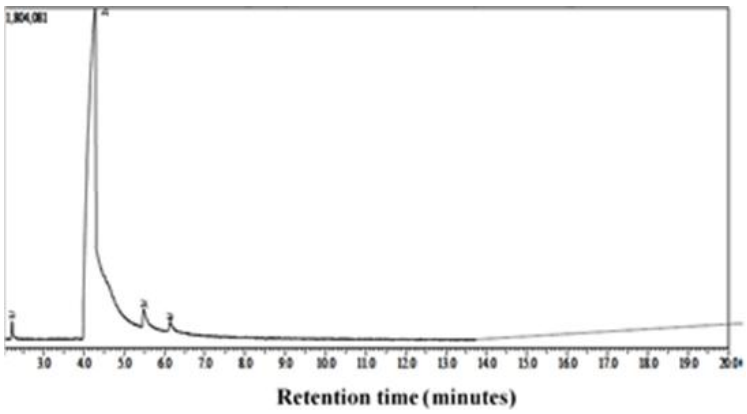

Figure 14. GC chromatogram of the final 1,2-propanediol-rich fraction

Table 8. Reported ^{1}H NMR assignments for 1,2-propanediol

Peak	Chemical shift (ppm)	Multiplicity	Assignment
a	1.14	Doublet	3H, -CH-CH_3
b	3.41	Doublet	2H, HO-CH_2-CH
c	3.74-3.78	Multiplet	1H, CH_2-CH-CH_3
d	4.90	Singlet	Exchangeable hydroxyl region

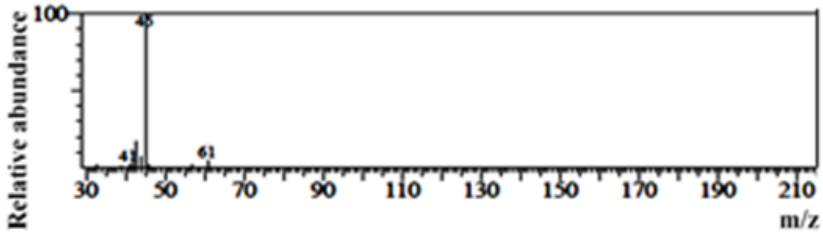

Figure 15. Mass spectrum of the final 1,2-propanediol-rich fraction

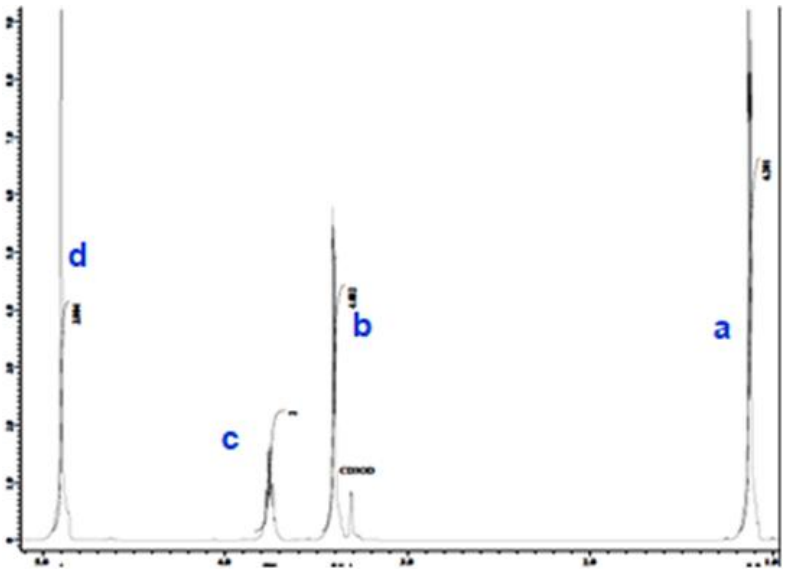

Figure 16. ^{1}H NMR spectrum of the final 1,2-propanediol-rich fraction

The reported 96.82% area value was higher than the intermediate purity, suggesting that esterification, extraction, hydrolysis, and final concentration also removed part of the earlier impurity mixture.

DISCUSSION

The 10.38% crude-glycerol recovery is chemically plausible for triglyceride transesterification because one glycerol molecule is released for every three fatty-acid methyl esters formed. The observed value also indicates that phase recovery was effective at laboratory scale. Feedstock free-fatty-acid content, catalyst dose, washing, and methanol recovery alter both the amount and the quality of the glycerol stream (Attarbachi et al., 2023a; (Rosmini et al., 2026).

Sulfuric-acid treatment was effective as a first purification step because it addressed two dominant alkaline-process impurities: residual base and soap. The reported 95.80% GC-area purity is substantially higher than would be expected for untreated crude glycerol. This agrees with the accepted mechanism of acidification, in which potassium soaps are protonated to free fatty acids and KOH is converted to sulfate salts. Yet GC area normalization preferentially describes volatile or chromatographable organic components. It cannot independently quantify water or non-volatile ash. Consequently, the broad O-H envelope and the 1643 cm^{-1} water-associated band should be interpreted together with the chromatogram: the organic fraction was glycerol-rich, but the total material may still have contained water and inorganic residue.

This distinction is central to downstream conversion. Gatti et al. (2023) showed that impurities in industrial crude glycerol can alter activity, selectivity, and stability during catalytic conversion to bio-propylene glycol. Water changes phase behavior and esterification equilibrium; salts can promote corrosion, foaming, or unwanted catalysis; fatty materials can foul heated surfaces; and residual methanol changes volatility and may participate in side reactions.

Recent purification reviews divide processes into physicochemical treatment, adsorption, membranes, ion exchange, and thermal separation. Acidification is comparatively simple and can be suitable as pretreatment, but reaching a high-value grade often requires a polishing operation. Attarbachi et al. (2023a) noted that technologies should be judged by recovery and impurity-specific removal as well as final glycerol content. Bansod et al. (2025) compared membrane, vacuum-distillation, and ion-exchange pathways and found that their economic performance differed because energy, chemicals, product recovery, and resilience to market changes were not equivalent.

The intermediate assignment deserves particular attention because dehydration of glycerol is known to produce a network of oxygenated products. The reported terminal-alkene FTIR bands and the ^{1}H NMR signals at approximately 5.16, 5.26, and 6.00 ppm are internally consistent with an allylic alcohol. The molecular formula of prop-2-en-1-ol also explains a strong m/z 57 fragment. These observations make the assignment reasonable. At the same time, the 83.66% GC area indicates a significant secondary fraction, and the method

intentionally used NaOH to reduce acrolein or related acidic/aldehydic material. The analytical package therefore supports an enriched prop-2-en-1-ol fraction.

Quantitative ^{1}H NMR with an internal standard would independently estimate assay and help distinguish the desired allylic alcohol from compounds with overlapping retention. Coupling constants would also strengthen the vinyl assignment because cis, trans, and geminal couplings provide structural information beyond chemical shift.

The high distillation temperature is both a mechanistic driver and a process limitation. The original observations that overly slow heating caused darkening and increased aldehydic products are consistent with thermal side reactions and polymerization of reactive dehydration products. Modern glycerol-valorization research generally seeks catalysts that lower activation barriers and control selectivity under milder conditions. Pandey & Biswas (2023) and Ma et al. (2023) show that catalyst design is directed toward balancing dehydration and hydrogenation while suppressing C-C cleavage, over-reduction, and coke. In comparison, the present process uses simple reagents and no compressed hydrogen but expends substantial thermal energy and requires repeated fractionation.

Formation of the formic ester was supported by the appearance of a 1728 cm^{-1} carbonyl band and a 1172 cm^{-1} C-O band. The disappearance of the ester carbonyl after alkaline treatment, together with reappearance of a broad diol O-H band, provides a coherent reaction sequence. The final NMR pattern is also structurally persuasive: a methyl doublet, oxygenated methylene, and oxygenated methine are the characteristic proton environments expected for 1,2-propanediol. Because hydroxyl protons exchange rapidly in CD_3OD, the signal near 4.90 ppm should be assigned cautiously; the nonexchangeable methyl, methylene, and methine signals provide stronger structural evidence.

The reported final yield of 77.73% compares favorably as a laboratory recovery through an addition-hydrolysis sequence, particularly because the intermediate was only 83.66% by GC area. Direct comparison with catalyst studies must be cautious because terms such as conversion, selectivity, isolated yield, and GC area are not equivalent. Luo et al. (2023) reported 1,2- or 1,3-propanediol yields between 51.2% and 82.5% depending on transition-metal modification of Pt/TiO2. Those values arise from a catalytic glycerol-hydrogenolysis framework with a defined feed and catalyst, whereas the present 77.73% is an isolated-process yield after multiple separation steps.

Recent reviews indicate that copper-containing catalysts remain central to selective 1,2-propanediol formation because Cu tends to favor C-O hydrogenolysis and shows lower activity for undesired C-C rupture than some noble metals. Nickel can enhance hydrogen activation but may promote deeper hydrogenolysis unless moderated by support properties and Cu addition. Ghorbani et al. (2025) therefore studied bimetallic Ni-Cu systems on different supports, while Hassenstein et al. (2026) developed a multifunctional Ru-Cu/CNT catalyst with very high selectivity. These advances illustrate the present research direction: integrating acid-base and metal functions in a controlled solid catalyst rather than relying only on severe temperature or soluble reagents.

A benefit of the formate-mediated route is avoidance of an external high-pressure hydrogen cylinder during the reported synthesis. This may simplify small-laboratory operation. Nevertheless, absence of compressed hydrogen does not automatically imply lower environmental impact. The process uses excess formic acid, sulfuric acid, KOH, ethanol, dichloromethane, drying salts, repeated extraction, and heating up to 260^0C. The resulting neutralization salts and solvent-recovery demand must be included in any sustainability claim. Sun et al. (2022) showed that energy, process economics, and environmental performance can change the preferred glycerol-to-propylene-glycol route even when reaction yield appears attractive.

Table 9. Position of the reported pathway within recent 1,2-propanediol research

Reference	Route or focus	Principal relevance to this study
Liu et al. (2021)	In-situ hydrogen generation over Pd-Cu catalyst	Demonstrates a route without externally supplied molecular hydrogen
Okolie (2022)	Renewable propylene-glycol pathways and industrial applications	Frames technology readiness, mechanisms, and scale-up challenges
Pandey & Biswas (2023)	Catalyst development for liquid- and vapor-phase hydrogenolysis	Shows the central role of catalyst acidity, metal function, and operating conditions
Luo et al. (2023)	Transition-metal-doped Pt/TiO2	Illustrates control of 1,2- versus 1,3-propanediol selectivity
Gatti et al. (2023)	Effect of crude-glycerol impurities	Supports impurity-specific feed characterization before conversion
Ghorbani et al. (2025)	Bimetallic Ni-Cu catalysts on different supports	Represents current optimization of metal-support synergy
Hassenstein et al. (2026)	Multifunctional Ru-Cu/CNT catalyst	Represents recent pursuit of near-complete selectivity and kinetic control

The 96.82% main-peak area is a strong indication that 1,2-propanediol was the dominant GC-detectable component, but detector response varies among compounds, and a peak-area percentage assumes comparable response factors.

Food-grade evaluation demands special attention to glycols that may have similar physical properties but different toxicological significance. Residual

methanol, dichloromethane, ethanol, formic acid or formate, and inorganic residues must also be quantified.

The humectant and solvent functions of 1,2-propanediol derive from its two hydroxyl groups, water miscibility, low volatility, and ability to dissolve flavouring or color components. The final FTIR and NMR data confirm the structural features responsible for these functions.

The 77.73% isolated yield and 96.82% GC area are promising inputs, but capital and operating estimates require batch time, equipment size, solvent recycle, heat integration, labor, product losses, and the cost of final polishing. Bansod et al. (2025) found that purification options respond differently to utility and product-price changes.

CONCLUSIONS AND RECOMMENDATIONS

Palm-oil transesterification produced a recoverable crude-glycerol phase that was upgraded by sulfuric-acid treatment. The purified glycerol was reported at 89.80% yield and 95.80% chromatographic purity. Subsequent conversion produced a fraction assigned as prop-2-en-1-ol at 75.13% yield and 83.66% purity, followed by 1,2-propanediol at 77.73% yield and 96.82% GC-area purity. FTIR, GC-MS, and 1H NMR features were broadly consistent with the proposed functional-group changes and final diol structure.

The evidence supports the conclusion that a 1,2-propanediol-rich product was obtained. The main recommendation is to add validated quantitative GC or HPLC using an authentic 1,2-propanediol standard and internal standard, Karl Fischer water determination, inorganic residue and ion analysis, residual-solvent testing, targeted ethylene-glycol and diethylene-glycol analysis, and replicate mass balances.

ADVANCED RESEARCH

Future research should compare the proposed formate-mediated route with catalytic hydrogenolysis under the same glycerol feed, system boundary, and product specification. Reaction intermediates should be monitored by time-resolved GC-MS and quantitative NMR, and prop-2-en-1-ol should be confirmed by co-injection with an authentic standard. Process intensification should focus on reducing the 260 ^{0}C thermal duty, solvent use, salt generation, and product losses. Finally, a cradle-to-gate life-cycle assessment, techno-economic evaluation, and food-grade hazard analysis are needed before scale-up.

ACKNOWLEDGMENT

The authors gratefully acknowledge the Institute for Research and Community Services (LPPM) Universitas Terbuka, Indonesia and MP3EI for financial support. This funding supported the experimental work, data analysis, and preparation of this manuscript.

REFERENCES

Attarbachi, T., Kingsley, M. D., & Spallina, V. (2023a). New trends on crude glycerol purification: A review. *Fuel*, *340*, 127485. https://doi.org/10.1016/j.fuel.2023.127485

Attarbachi, T., Kingsley, M. D., & Spallina, V. (2023b). New trends on crude glycerol purification: A review. *Fuel*, *340*, 127485. https://doi.org/10.1016/j.fuel.2023.127485

Bansod, Y., Crabbe, B., Forster, L., Ghasemzadeh, K., & D'Agostino, C. (2024). Evaluating the environmental impact of crude glycerol purification derived from biodiesel production: A comparative life cycle assessment study. *Journal of Cleaner Production*, *437*, 140485. https://doi.org/10.1016/j.jclepro.2023.140485

Bansod, Y., Ghasemzadeh, K., & D'Agostino, C. (2025). Techno-economic assessment of biodiesel-derived crude glycerol purification processes. *RSC Sustainability*, *3*(6), 2605–2618. https://doi.org/10.1039/D4SU00599F

Gatti, M., Pompeo, F., Nichio, N., & Santori, G. (2023). Crude Glycerol Hydrogenolysis to Bio-Propylene Glycol: Effect of Its Impurities on Activity, Selectivity and Stability. *Processes*, *11*(6), 1731. https://doi.org/10.3390/pr11061731

Ghorbani, A., Boahene, P., & Dalai, A. K. (2025). Enhanced 1,2-propanediol production from glycerol using bimetallic Ni–Cu catalysts on different supports. *Sustainable Energy & Fuels*, *9*(20), 5657–5672. https://doi.org/10.1039/D5SE00480B

Główka, M., & Krawczyk, T. (2023). New Trends and Perspectives in Production of 1,2-Propanediol. *ACS Sustainable Chemistry & Engineering*, *11*(19), 7274–7287. https://doi.org/10.1021/acssuschemeng.3c01018

Hassenstein, P., Niehaus, D., Taherkhani, N., Krueger, J.-D. H., Voß, D., Lumpp, D., Schroeter, B., Paschalidis, L., Smirnova, I., Skiborowski, M., & Albert, J.

(2026). Boosting the Chemical Hydrogenolysis of Glycerol to 1,2-Propanediol to Almost Perfect Selectivity Using a Multifunctional Ru–Cu Carbon-Nanotube-Supported Catalyst. *ACS Sustainable Chemistry & Engineering*, *14*(15), 7559–7574. https://doi.org/10.1021/acssuschemeng.6c02083

Lewis, A. S., Boomhower, S. R., Marsh, C. M., & Jack, M. M. (2024). Considerations for deriving a safe intake of propylene glycol. *Food and Chemical Toxicology*, *186*, 114460. https://doi.org/10.1016/j.fct.2024.114460

Liu, Y., Wu, M., Rempel, G. L., & Ng, F. T. T. (2021). Glycerol Hydrogenolysis to Produce 1,2-Propanediol in Absence of Molecular Hydrogen Using a Pd Promoted Cu/MgO/Al2O3 Catalyst. *Catalysts*, *11*(11), 1299. https://doi.org/10.3390/catal11111299

Luo, H., Sun, G., shi, Y., Shen, Y., & Xu, K. (2014). Evaluation of the Di(2-ethylhexyl) phthalate released from polyvinyl chloride medical devices that contact blood. *SpringerPlus*, *3*(1), 58. https://doi.org/10.1186/2193-1801-3-58

Luo, Z., Zhu, Z., Xiao, R., & Chu, D. (2023). Selective Production of 1,2-Propanediol or 1,3-Propanediol from Glycerol Hydrogenolysis over Transition Metal Doped Pt/TiO $_2$. *Chemistry – An Asian Journal*, *18*(3). https://doi.org/10.1002/asia.202201046

Ma, L., Liu, H., & He, D. (2023). Recent Progress in Catalyst Development of the Hydrogenolysis of Biomass-Based Glycerol into Propanediols—A Review. *Bioengineering*, *10*(11), 1264. https://doi.org/10.3390/bioengineering10111264

Okolie, J. A. (2022). Insights on production mechanism and industrial applications of renewable propylene glycol. *IScience*, *25*(9), 104903. https://doi.org/10.1016/j.isci.2022.104903

Pandey, D. K., & Biswas, P. (2023). Review of the Development of Heterogeneous Catalysts for Liquid and Vapor Phase Hydrogenolysis of Glycerol to Propylene Glycol (1,2-Propanediol): State-of-the-Art and Outlook. *Energy & Fuels*, *37*(10), 6879–6906. https://doi.org/10.1021/acs.energyfuels.2c03806

Rosmini, C., Mitrev, Y., & Dimitrov, M. (2026). The Crude Glycerol Challenge: Purification Technologies and Possible Valorization Pathways in the Biodiesel Industry. *Molecules*, *31*(11), 1841. https://doi.org/10.3390/molecules31111841

Sun, P., Zhang, W., Yu, X., Zhang, J., Xu, N., Zhang, Z., Liu, M., Zhang, D., Zhang, G., Liu, Z., Yang, C., Yan, W., & Jin, X. (2022). Hydrogenolysis of Glycerol to Propylene Glycol: Energy, Tech-Economic, and Environmental Studies. *Frontiers in Chemistry*, *9*. https://doi.org/10.3389/fchem.2021.778579

Tran, N. L., Anderson, M. M., & Jack, M. M. (2025). Tiered intake assessment for propylene glycol in beverages. *Food Additives & Contaminants: Part A*, *42*(3), 317–325. https://doi.org/10.1080/19440049.2025.2449820